Spectrochimica Acta Part A: Molecular and Biomolecular Spectroscopy 121 (2014) 230–237

Contents lists available at ScienceDirect

Spectrochimica Acta Part A: Molecular and Biomolecular Spectroscopy

journal homepage: www.elsevier.com/locate/saa

Insights into the selective binding and toxic mechanism of microcystin to catalase

Yuandong Hu [a,b], Liangjun Da [a,*]

[a] Department of Environmental Science, East China Normal University, Shanghai 200062, China
[b] Department of Landscape, Northeast Forestry University, Harbin 150040, China

HIGHLIGHTS

- Interaction of catalase and microcystin was studied.
- Binding of microcystin to catalase follows the electrostatic force.
- Conformational alterations of catalase were caused by microcystin binding.
- Activity of catalase was inhibited by noncompetitive mechanism.

GRAPHICAL ABSTRACT

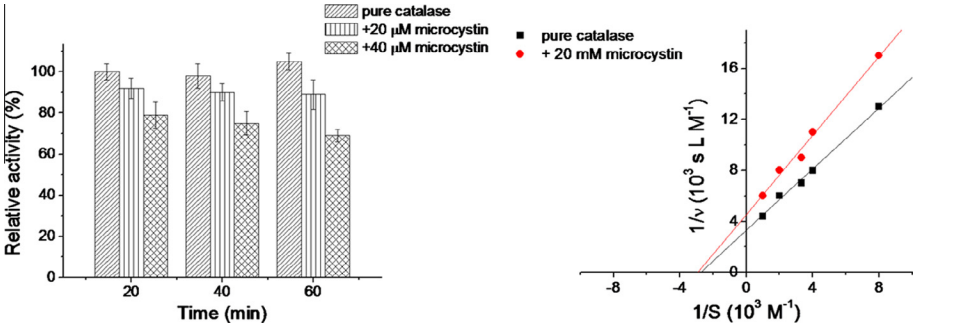

ARTICLE INFO

Article history:
Received 4 June 2013
Received in revised form 22 August 2013
Accepted 25 September 2013
Available online 19 October 2013

Keywords:
Cyanotoxin
Catalase
Fluorescence quenching
FT-IR
Enzymatic inhibition

ABSTRACT

Microcystin is a sort of cyclic nonribosomal peptides produced by cyanobacteria. It is cyanotoxin, which can be very toxic for plants and animals including humans. The present study evaluated the interaction of microcystin and catalase, under physiological conditions by means of fluorescence, three-dimensional (3D) fluorescence, circular dichroism (CD), Fourier Transform infrared (FT-IR) spectroscopy, and enzymatic reactionkinetic techniques. The fluorescence data showed that microcystin could bind to catalase to form a complex. The binding process was a spontaneous molecular interaction procedure, in which electrostatic interactions played a major role. Energy transfer and fluorescence studies proved the existence of a static binding process. Additionally, as shown by the three-dimensional fluorescence, CD and FT-IR results, microcystin could lead to conformational and microenvironmental changes of the protein, which may affect the physiological functions of catalase. The work provides important insights into the toxicity mechanism of microcystin *in vivo*.

Introduction

Cyanobacteria (formerly called "blue–green algae") have a worldwide distribution and can form extensive blooms in freshwater and estuarine habitat. Factors that contribute to bloom formation and toxin production include warm water [1], nutrient enrichment [2] and seasonal increases in light intensity [3]. Rising global temperatures and eutrophication may contribute to more frequent events and cyanobacterial "super-blooms", with enhanced risks to human health [4]. Recently, *Microcystis* bloom frequently occurred in the eutrophic lakes at Daqing, Heilongjiang Province, China and the dominant species is *Microcystis aeruginosa*, which produces a family of related cyclic heptapeptides (mainly microcystins) [5]. These toxins are severely hepatotoxic, are produced in *Microcystis* cells and are released into water body when cyanobacterial cells are broken.

Microcystin (shown in Fig. 1) is one of over 80 known toxic variants and is the most studied by chemists, pharmacologists, biologists and ecologists. Microcystin-containing "blooms" are a problem worldwide, including China, Brazil, Australia, the United States and much of Europe [6]. Toxic blooms of cyanobacteria have

* Corresponding author. Tel.: +86 021 54341272.
E-mail address: dalj@sh163.net (L. Da).

1386-1425/$ - see front matter
http://dx.doi.org/10.1016/j.saa.2013.09.078

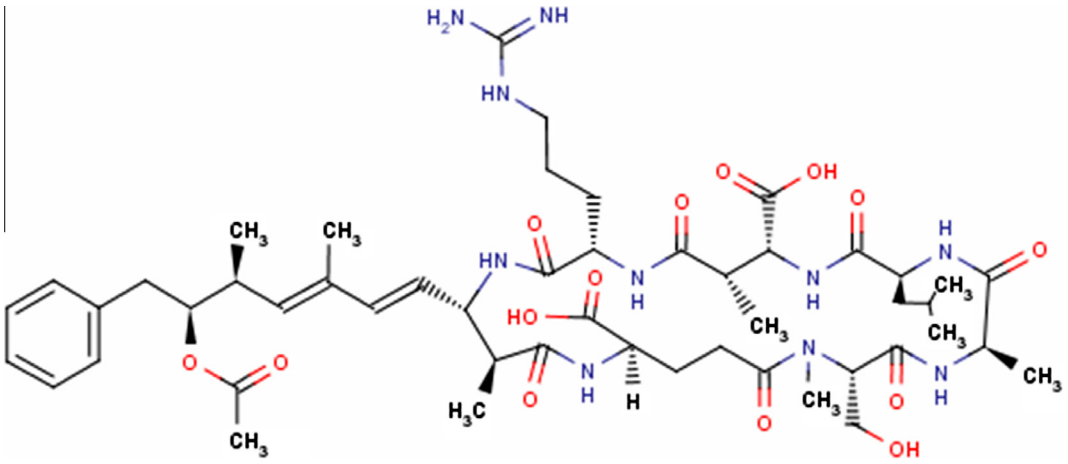

Fig. 1. Molecular structure of microcystin.

been associated with acute hepatotoxicity in various species of domestic animals and humans. Once ingested, microcystin travels to the liver, via the bile acid transport system, where most is stored; though some remains in the blood stream and may contaminate tissue [7,8]. Microcystin binds covalently to protein phosphatases thus disrupting cellular control processes. In addition, epidemiologic studies in China have suggested that microcystins in contaminated water may play a role in the higher incidences of primary human hepatocellular carcinomas in many areas, particularly in Daqing, China [5].

Detoxification is one of the liver's functions. Catalase catalyzes the breakdown of hydrogen peroxide, which is toxic (It is highly reactive so can cause cell damage. It comes from the small intestine via the portal vein, from things we eat or drink, e.g. alcohol) to oxygen and water, which are harmless. When the catalase structure is altered and the function is impeded, liver could not work normally. Thus to elucidate the interaction of catalase and microcystin is of great importance to get the insight of the toxic mechanism of microcystin [9–12]. However, there has been no report regarding the toxic effects of microcystin on catalase.

The interaction of microcystin with catalase was investigated under physiological condition in phosphate buffered saline (PBS) buffer solution at pH 7.4 by means of various spectroscopic methods (fluorescence, CD and FT-IR) and enzymatic reactionkinetic technique. Binding constants and the number of binding sites were calculated using Stern–Volmer equations. The thermodynamic parameters are calculated and discussed. The distance r between donor (catalase) and acceptor (microcystin) was obtained according to fluorescence resonance energy transfer and the alterations of catalase secondary structure induced by microcystin were confirmed by 3D fluorescence, FT-IR and CD measurements.

Materials and methods

Catalase was purchased from Sinopharm Chemical Reagent Beijing Co., Ltd. (Beijing, China). Microcystin with 98% purity was donated by Shanghai Institute of Pharmaceutical Industry, China. All other reagents of analytical grade were used and they were bought from Nanjing Di'an Biotechnology Co., Ltd., China. Double-distilled water was used throughout the experiments. Catalase was dissolved in 0.05 M phosphate buffered saline (PBS) solution to form a 2.0×10^{-6} M solution and then preserved at 4 °C for later use.

Steady state fluorescence spectra were acquired on a Hitachi F4010 (Hitachi, Tokyo, Japan) using 1 cm matched quartz cuvettes keeping excitation and emission slit widths of 3 nm. Intrinsic fluorescence of catalase was measured by exciting at 280 nm. Temperature dependent fluorescence spectral studies were performed on the Hitachi unit equipped with a circulating water bath. For Stern–Volmer calculations, the fluorescence data were processed with considerations of inner filter effects [11], which would cause absorption of both excitation and emission radiation. Methods to inner filter effect corrections are taken from Ding [13].

The conformational changes in the protein secondary structures on microcystin binding were studied using a Jasco J815 spectropolarimeter (Shimadzu, Tokyo, Japan) at 25 °C equipped with a Peltier cell holder and temperature controller PFD425 L/15. The protein concentration and path length of the cells used were 2×10^{-7} M and 0.1 cm for far UV CD. Secondary structure calculations were performed using the software supplied by Jasco Company.

The absorbance spectra of microcystin in phosphate buffer solution were recorded on a Shimadzu UV2450 spectrophotometer (Shimadzu, Tokyo, Japan). Slit width and scanning speed were set at 2 nm and 100 nm/min, respectively.

FT-IR measurements were carried out on Perkin Elmer Spectrum GX FTIR Spectrometer (Perkin Elmer, Shelton, CT) equipment using ZnSe window. Hundred scans were recorded for each sample in the spectral range of 400–4000 cm^{-1} with a resolution of 4 cm^{-1}. The background was corrected before scanning the samples and the buffer spectrum collected. FT-IR spectra of free catalase (5×10^{-4} M) and catalase–microcystin complex (1:2) were recorded to identify changes in secondary structure in catalase on interaction with microcystin. All the experiments were performed at room temperature (25 °C).

The activity of catalase was measured using H_2O_2 as the substrate. Catalase can catalyze H_2O_2 into water and oxygen. The enzyme activity was obtained based on the decrease in absorbance at 400 nm, where H_2O_2 absorbs, in buffered phosphate medium (pH 7.4) containing various concentration of microcystin. One unit of CAT activity is defined as the amount of enzyme that decomposes 1 mmol H_2O_2 per minute. The final amount of catalase and H_2O_2 are 5×10^{-6} M and 8 mM, respectively. The inhibition mechanism was determined using the methods from Lineweaver [14] and the experimental conditions are the same with the activity measurements.

Results and discussion

Fluorescence quenching mechanism of catalase by microcystin

The fluorescence of protein originates mainly from the amino acid residues of tryptophan (Trp) or tyrosine (Tyr), and

fluorescence quenching measurement can provide rich information for the interaction between pollutant molecules and proteins, such as, binding constant, number of binding site, binding location and binding mechanism.

Fig. 2 shows the fluorescence quenching spectra of catalase induced by different concentrations of microcystin in phosphate buffer solution with pH 7.4 at the excitation wavelength of 280 nm. It can be observed that the fluorescence intensities of catalase gradually decreased accompanying with red shifts of the maximum emission bands from 342 nm to 344 nm when $C_{microcystin}/C_{catalase}$ increased from 0 to 6. The significant fluorescence quenching of the protein demonstrated that microcystin has been bound with the protein, and the obvious blue shifts of the emission bands indicated that the conformation of the protein has been changed and the Trp residues of the protein were exposed to more nonpolar environment after interacting with microcystin [13].

The Stern–Volmer equation (Eq. (1)) was used to calculate the Stern–Volmer quenching constant K_{SV} and the bimolecular quenching rate constant K_q [15]:

$$F_0/F = 1 + K_q\tau_0[Q] = 1 + K_{SV}[Q] \quad (1)$$

F_0 and F represent the fluorescence intensities of a protein in the absence and presence of the ligand, $[Q]$ is the drug concentration, and τ_0 is the average lifetime of the fluorophore in the absence of the ligand.

Fig. 3A and B presents the Stern–Volmer curves for the fluorescence quenching of catalase after interacting with different concentrations of microcystin at pH 7.4. It can be seen from Fig. 3A that the Stern–Volmer curves were linear when the molar ratio of the drug to protein ranged from 0 to 6 at pH 7.4. The bimolecular quenching rate constant (K_q) obtained at 298 K according to Eq. (1) was $1.12 \times 10^{13}\ M^{-1}\ s^{-1}$ (Table 1), which showed that K_q was much higher than the limiting diffusion constant K_d ($K_d = 2 \times 10^{10}$ - $M^{-1}\ s^{-1}$) of the biomolecule, These results demonstrated that the fluorescence quenching of catalase by microcystin was mainly a static quenching process, and the complexes of pollutant and protein have been formed.

Since the fluorescence quenching is a static process, the number of the binding site (n) and the binding constants (K_A) can be obtained by Eq. (2) deduced in previous reports [16–18]:

$$\lg\frac{F_0 - F}{F} = \lg K_A + n\lg[Q]. \quad (2)$$

The n values from the slopes of Eq. (2) was 0.949 at 298 K (Table 2), indicating that one molecule of microcystin bound with one molecule of catalase. The binding constant of microcystin decreased with increasing temperature, indicating that microcystin–catalase was not moderate and sensitive to temperature.

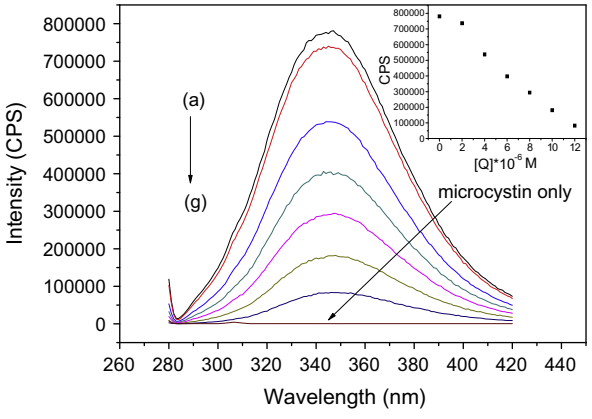

Fig. 2. Fluorescence emission spectra of catalase in the presence of microcystin. $C_{catalase}$: 2×10^{-6} M, $C_{microcystin}$, a–g: 0, 2, 4, 6, 8, 10 and 12×10^{-6} M; pH 7.4, T = 298 K.

Interaction forces between quencher and biomolecules may include hydrophobic force, electrostatic interactions, van der Waals interactions, hydrogen bonds, and others [19]. In order to map the interaction between microcystin and catalase, the thermodynamic parameters were calculated using the Van't Hoff equation:

$$\ln\left(\frac{K_2}{K_1}\right) = \frac{\Delta H^\circ}{R}\left(\frac{1}{T_1} - \frac{1}{T_2}\right) \quad (3)$$

where K is the binding constant to a site, R is the universal gas constant (8.314 J mol^{-1} K^{-1}), ΔH and ΔS° are the changes in enthalpy and entropy during quenching process. The free energy change (ΔG°) associated with the interaction of microcystin and catalase can be calculated from the following equation:

$$\Delta G^\circ = \Delta H^\circ - T\Delta S^\circ = -RT\ln K^\circ \quad (4)$$

According to the binding constants that were found at three temperatures above (291 K, 298 K and 305 K), the change in enthalpy (ΔH°) and entropy (ΔS°) values were obtained from Van't Hoff equation, and the results are presented in Table 3. The free energy change ΔG° was calculated with the Eq. (4). As Table 3 shown, the ΔH° and ΔS° for the binding reaction between microcystin and catalase were found to be -9.79×10^3 J mol^{-1} and 58.8 J mol^{-1} K^{-1} at 298 K. The negative ΔG° corresponded to a spontaneous binding process. Therefore, the binding process between microcystin and catalase was spontaneous.

Different signs and magnitude for the thermodynamic parameters appeared with different interaction forces, such as typical hydrophobic interactions of positive ΔH° and ΔS°, van der Waals force and hydrogen bonding formation showing with negative ΔH° and ΔS° in low dielectric media, and electrostatic interactions playing a role in negative ΔH° and positive ΔS°. Therefore, the interaction forces behind the binding of microcystin with catalase may derive from electrostatic interactions because of the negative ΔH° and positive ΔS° (Table 3). Meanwhile, the negative ΔH° values indicated that the formation of catalase–microcystin coordination compound was an exothermic reaction.

Energy transfer to microcystin and the binding distance measurement

Fluorescence resonance energy transfer (FRET) is a good technique to determine the distance of separation between the donor (fluorophore) and the acceptor. The FRET efficiency depends on the extent of overlap of the donor emission and acceptor absorption, orientation of the transition dipole of the donor, and the distance between the donor and acceptor which must be within the Forster distance of 2–8 nm [20]. The overlap of the absorbance spectrum of microcystin with the emission spectra of catalase–microcystin was presented in Fig. S1 (Supplementary Information). In a proteinous environment, the proximity of the ligand molecule to the Trp moiety is often determined through FRET study. The efficiency (E) of the FRET process depends on the inverse sixth power of the average distance between donor and acceptor (r) and of the critical energy transfer distance or Forster radius (R_0). When the efficiency of transfer is 50%, a condition of 1:1 situation of donor to acceptor concentration prevails and E is expressed by the equation [21]:

$$E = 1 - \frac{F}{F_0} = \frac{R_0^6}{R_0^6 + r^6} \quad (5)$$

R_0 can be calculated using the relationship [22]:

$$R_0^6 = 8.8 \times 10^{-25} k^2 N^{-4} \Phi J \quad (6)$$

where k^2 is the spatial factor of orientation, n is the refractive index of the medium, Φ is the fluorescence quantum yield of the donor

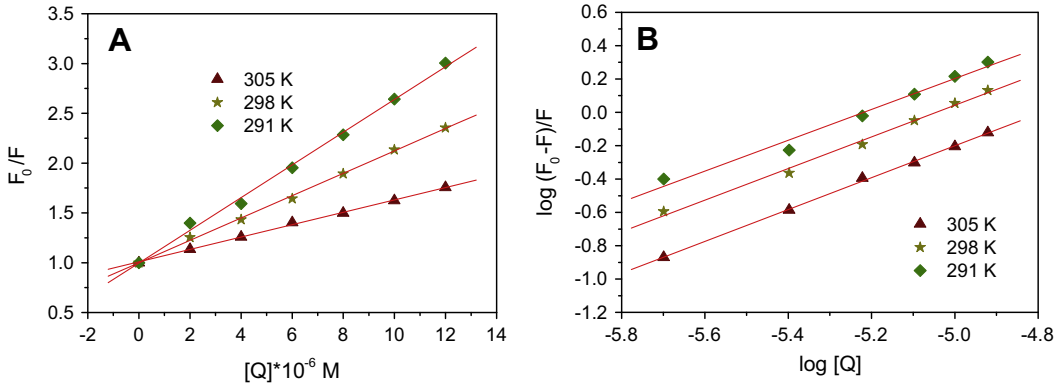

Fig. 3. (A) Stern–Volmer and (B) Hill plots of fluorescence data at different temperatures.

Table 1
Stern–Volmer quenching constants of the catalase–microcystin system at different temperatures.

T (K)	K_q (M^{-1} s^{-1})	K_{SV} (M^{-1})	R[a]	SD[b]
291	1.64×10^{13}	1.64×10^{5}	0.9980	0.04875
298	1.12×10^{13}	1.12×10^{5}	0.9992	0.02182
305	0.62×10^{13}	0.62×10^{5}	0.9992	0.01144

[a] The correlation coefficient.
[b] The standard deviation.

Table 2
Binding parameters of the catalase–microcystin system at different temperatures.

T (K)	K_A (M^{-1})	n	R[a]	SD[b]
291	6.73×10^{4}	0.925	0.9904	0.04151
298	6.12×10^{4}	0.949	0.9968	0.02465
305	3.79×10^{4}	0.956	0.9994	0.01095

[a] The correlation coefficient.
[b] The standard deviation.

Table 3
Thermodynamic parameters of the catalase–microcystin system.

T (K)	$\Delta G°$ (J mol^{-1})	$\Delta S°$ (J mol^{-1} K^{-1})	$\Delta H°$ (J mol^{-1})
291	-2.69×10^{4}		
298	-2.73×10^{4}	58.8	-9.79×10^{3}
305	-2.67×10^{4}		

and J is the overlap integral of the fluorescence emission spectrum for the donor and the absorption spectrum of the acceptor. J may be calculated from the equation [23]:

$$J = \frac{\sum F(\lambda)\varepsilon(\lambda)\lambda^4 \Delta\lambda}{\sum F(\lambda)\Delta\lambda} \quad (7)$$

where $F(\lambda)$ and $\varepsilon(\lambda)$ represent the fluorescence intensity of the donor and the molar absorption coefficient of the acceptor, respectively, at the wavelength λ. Using the values of $k^2 = 2/3$, $n = 1.36$ and $\Phi = 0.15$ for the protein, the values of E, J, R_0 and r have been calculated to be 0.09, 8.94×10^{-14} cm^3 M^{-1}, 2.62 nm and 2.86 nm for catalase–microcystin. The distance between ligand and Trp is far lower than the 7 nm value and $0.5R_0 < r < 1.5R_0$, indicating high probability of energy transfer from Trp of catalase to microcystin. This is also in accordance with static quenching mechanism. The results indicated that the conditions of Forster energy transfer for the binding is obeyed.

Conformational change studies by synchronous, CD, 3D fluorescence and FT-IR

Conformational changes occurring in the protein on binding were evaluated using synchronous fluorescence [24]. When the scanning interval between the excitation and emission wavelengths is stabilized at 15 and 60 nm, synchronous fluorescence of the protein is characteristic of Tyr and Trp residues; fluorescence quenching caused by the ligand implies alteration of the polarity around these residues. The effect of microcystin on the synchronous fluorescence of catalase with $\Delta\lambda = 15$ nm revealed that the fluorescence intensity diminished systematically with a blue shift of the maximum emission by 11 nm (Fig. 4). This phenomenon indicates that in presence of microcystin, Tyr residues are in a polar environment and are more exposed to solvent. Comparatively, there is almost no shift in the maximum emission wavelength when $\Delta\lambda = 60$ nm, showing that little microenvironmental change takes place around Trp residues. Therefore microcystin changed the polarity around Tyr slightly, while that around Trp was not changed, which is in agreement with the results from quenching and FRET experiments implicating unequivocally the involvement of Trp in the binding process.

The far ultraviolet CD spectrum (Fig. 5A) of native catalase contained two minima at 208 ($\pi \rightarrow \pi^*$) and 222 nm ($n \rightarrow \pi^*$), which are characteristic of α-helical structures [25,26]. The secondary structures of native catalase were found to contain 25.0% α-helix, 23.0% β-sheet, 23.0% turn and 29.1% random coils. Microcystin is an achiral molecule that is not CD active. Upon titrating with increasing concentrations of microcystin, the CD spectrum of catalase decreased in intensity without any shift in the negative peaks, indicating a slight decrease in the helical structure. At saturation, corresponding respectively to 0.4 μmol and 0.8 μmol of microcystin for catalase there was a reduction of 2% and 3.4% of α-helical structure (Table 4). Thus, the unfolding and loss of helical stability has been observed on binding, inducing secondary structural changes in the proteins [27,28].

The effects on the secondary structure are more prominent in the deconvoluted spectra of catalase (Fig. 5B) and the catalase–microcystin complex (Fig. 5C). The free protein contained 26% α-helix, 24% β-sheet, 26% turn and 26% random structure. The estimated content of different secondary structures in native catalase is consistent with those already reported in literature [29,30]. On interaction of microcystin with catalase, the α-helix content was reduced from 26% to 24%. A reduction in the α-helical content was also obtained from CD studies as discussed earlier. The β-sheet content increased from 24% to 27%. The random structure content remains same whereas turn structure decreased from 26% to 25%. The trend of changes in secondary structures by CD and FT-IR are

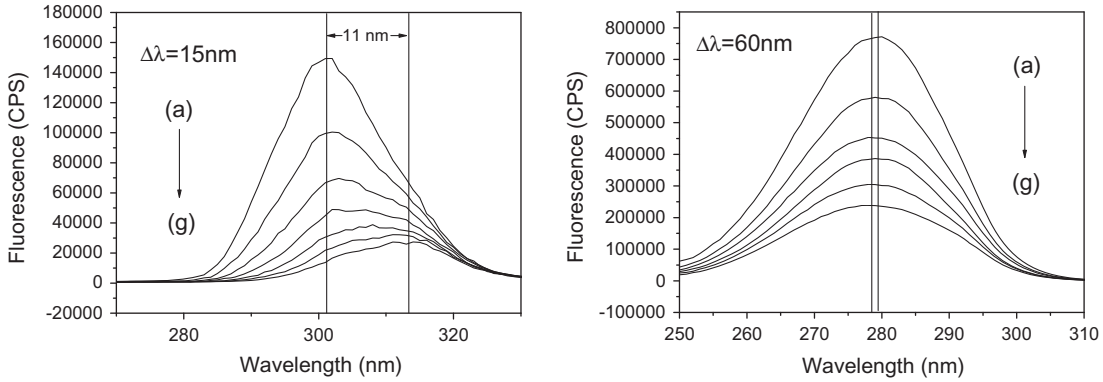

Fig. 4. Synchronous fluorescence spectra of catalase in the presence of microcystin at $\Delta\lambda$ = 60 nm and $\Delta\lambda$ = 15 nm. Experimental conditions are in agreement with Fig. 2.

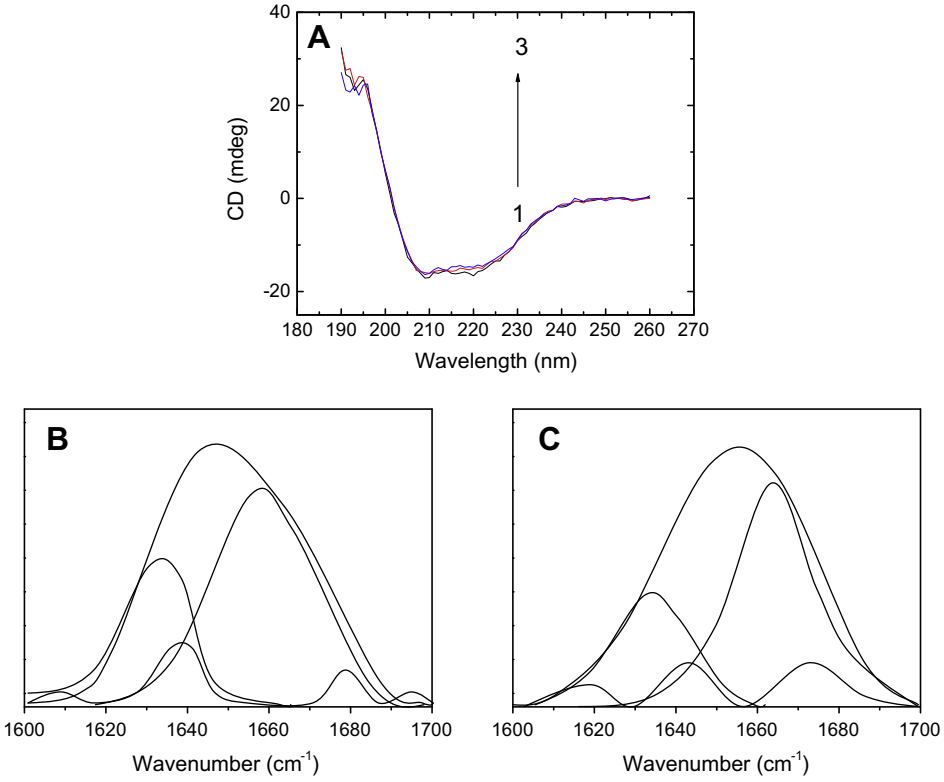

Fig. 5. (A) CD spectra of catalase–microcystin system obtained at room temperature and pH 7.4. $C_{catalase}$: 2×10^{-7} M, $C_{microcystin}$: 0, 4 and 8×10^{-7} M. Second-derivative resolution enhancement and curve-fitted amide I (1700–1600 cm^{-1}) region of the (A) free catalase, (B) catalase–microcystin. $C_{catalase}$: 2×10^{-4} M, $C_{microcystin}$: 4×10^{-4} M.

Table 4
Secondary structural content of catalase in the absence and presence of gemcitabine.

$C_{catalase}$:$C_{microcystin}$	Content (%)			
	α-helix (±2%)	β-sheet (±1%)	β-turn (±1%)	Random coil (±2%)
0	25.0	23.0	23.0	29.1
1:2	23.0	23.9	23.3	30.3
1:4	21.6	25.7	23.3	29.5

similar though the content of secondary structural elements differs as discussed below. Apart from differences in sample preparation for the two methods, where a hydrated film was used for FT-IR and an aqueous solution was used for CD measurements, a major difference lies in the spectroscopic signals themselves. FT-IR signals arise from the vibrational modes whereas CD spectra are obtained from electronic transitions that may be the cause for the difference in content of their structural information. Similar differences between FT-IR and CD spectroscopic results for proteins have been reported elsewhere [27,31].

The 3D fluorescence spectroscopy has been widely used in the analysis of proteins. It could be an important hint suggesting the changes in protein conformation if there are shifts, appearance or disappearance, and intensity changes of fluorescent peaks. Thus, it can comprehensively analyze the information of changes in protein conformation according to the fluorescent spectrum changes. Herein, the conformational and microenvironmental changes of catalase were investigated by comparing the spectral changes in the absence and presence of microcystin. As shown in Fig. 6 with the corresponding parameters shown in Table 5, Peak A is the Rayleigh scattering peak ($\lambda_{ex} = \lambda_{em}$) and the fluorescence intensity of Peak A increased with the addition of microcystin. Peak B is the

second-ordered scattering peak ($\lambda_{em} = 2\lambda_{ex}$). With the addition of microcystin, the fluorescence intensity of Peak A increased gradually. The reason for this phenomenon is that the formation of catalase–microcystin complex makes the diameter of the macromolecule increased, which in turn results in the enhancement of the scattering effect. With increasing concentration of microcystin, the fluorescence intensity of Peak 1 reduced significantly (from 7560 to 3498), which implied the obvious perturbation to the microenvironmental polarities of Trp and Tyr residues caused by the catalase–microcystin complex formation. Besides Peak 1, there is another strong fluorescence peak (Peak 2) that mainly represented the fluorescence characteristic of polypeptide backbone structures. The fluorescence intensity of Peak 2 decreased markedly (from 8721 to 3086) after the addition of microcystin, which indicated the conformational change of catalase induced by the binding activity of microcystin. This result was in accordance with the decrease of α-helix content in the CD spectra. Combined with the synchronous fluorescence, CD and FT-IR results, the decrease of fluorescence intensity of the two peaks implied that the interaction between microcystin and catalase induced a slight unfolding of the polypeptide backbone of the protein. The formation of catalase–microcystin complex probably resulted in the exposure of some hydrophobic regions and then brought about the conformational changes of catalase.

Effect of microcystin on catalase activity

The liver plays a large role in the detoxification of microcystins. As one of the main enzymes in hepatocytes, catalase may inevitably encounter microcystins and its activity may be influenced. Thus, study of catalase activity in hepatocytes has great significance for investigating the function of the enzyme. Catalase is a homo-tetrameric enzyme that has its heme active site deeply buried inside the protein [32]. Its only substrate, hydrogen peroxide (H_2O_2), reaches the heme through a 45 Å-long channel (Fig. 7). The structure of an enzyme is related to the function so that a structural variation may affect its normal physiological function [33]. It can be seen from the above data that the effect of microcystin on catalase conformation is obvious, and we investigated the effects of different concentrations of microcystin on the activity of catalase (Fig. 7). Catalase was exposed to graded concentrations of microcystin ranging from 10 to 100 mM for different time points. The range of concentrations could represent a health hazard. As shown in Fig. 8A, the relative catalase activities were reduced to 92% and 79% after treatment with 20 and 40 mM microcystin for 20 min, respectively. As the exposure time increased to 40 min, the activities were reduced to 90% and 75%. The incubation time has little effect on the activities of catalase after treatment with 20 mM microcystin. When catalase was incubated in 40 mM, the catalase activity decreased significantly with longer exposure time.

To confirm the inhibition mode, we drew the Lineweaver–Burk plots of catalase and catalase–microcystin systems (Fig. 8B). The Lineweaver–Burk plots with and without catalase intersect on the *x* axis, showing a typical feature of noncompetitive inhibition. Based on the Lineweaver–Burk plots, microcystin did not directly bind into the catalase activity site, but the binding of microcystin into the enzyme cavity influenced the microenvironment of the catalase activity site which resulted in the reduced catalase activity. Microcystin binds to a site beside the active site of catalase and

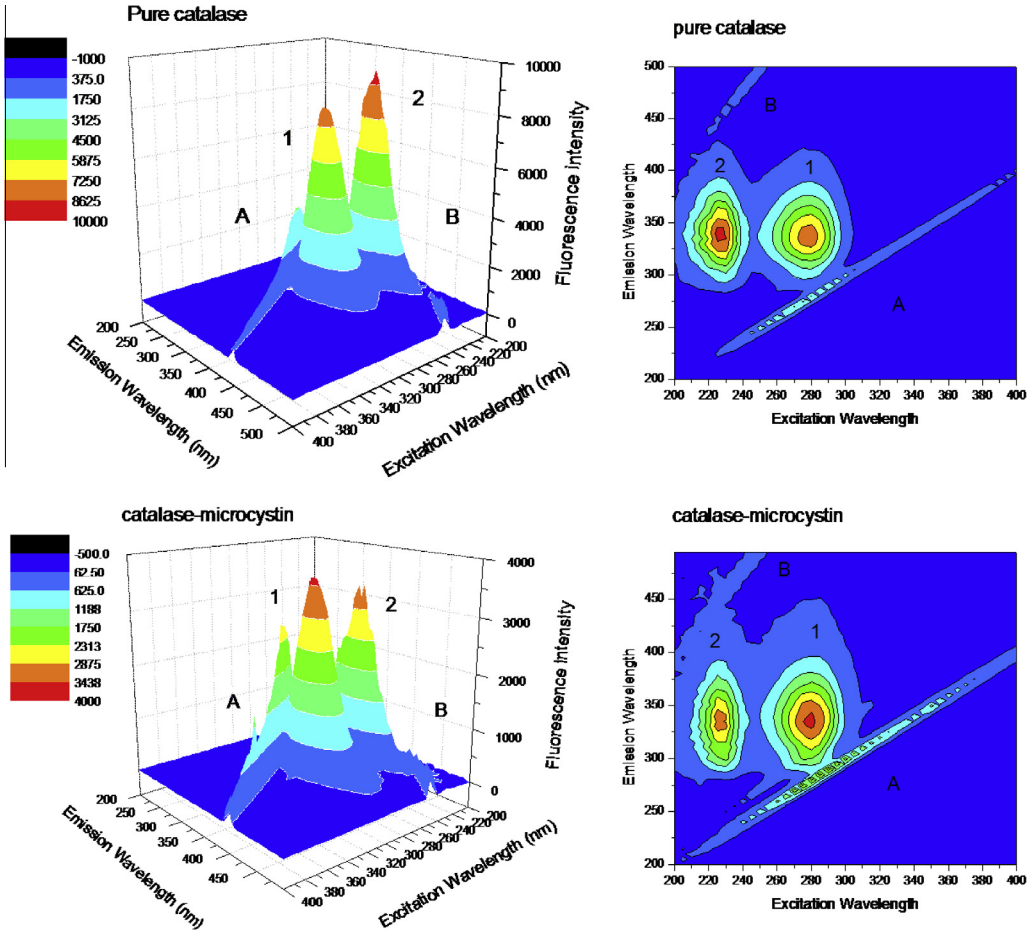

Fig. 6. The three-dimensional fluorescence spectra of (A) pure catalase and (B) catalase–microcystin complex. $C_{catalase}$: 2×10^{-6} M, $C_{microcystin}$: 8×10^{-6} M; pH 7.4, T = 298 K.

Table 5
Three-dimensional projections and the corresponding excitation–emission matrix fluorescence diagram of catalase–microcystin system.

Peaks	Pure catalase			Catalase–microcystin		
	Peak position $\lambda_{ex}/\lambda_{em}$ (nm/nm)	Stokes $\Delta\lambda$ (nm)	Fluorescence internsity	Peak position $\lambda_{ex}/\lambda_{em}$ (nm/nm)	Stokes $\Delta\lambda$ (nm)	Fluorescence internsity
A	$\lambda_{ex} = \lambda_{em}$	0	2534	$\lambda_{ex} = \lambda_{em}$	0	2743
B	$\lambda_{ex} = 2\lambda_{em}$	0	849	$\lambda_{ex} = 2\lambda_{em}$	0	513
1	278/337	21	7560	278/337	23	3498
2	225/337	54	8721	225/337	75	3086

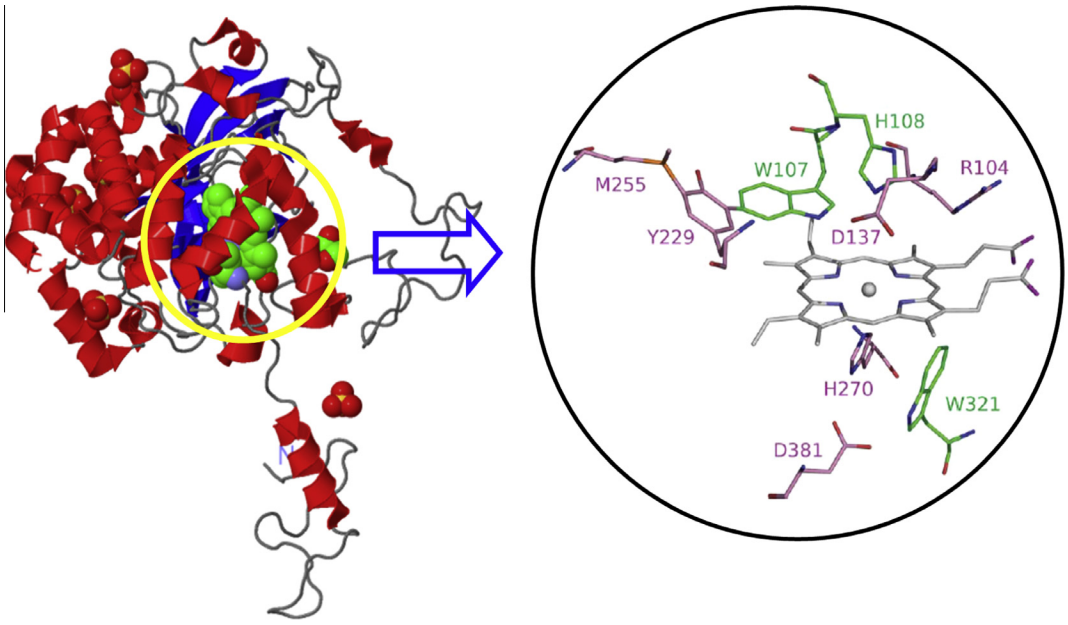

Fig. 7. Structure of catalase with activity site indicated.

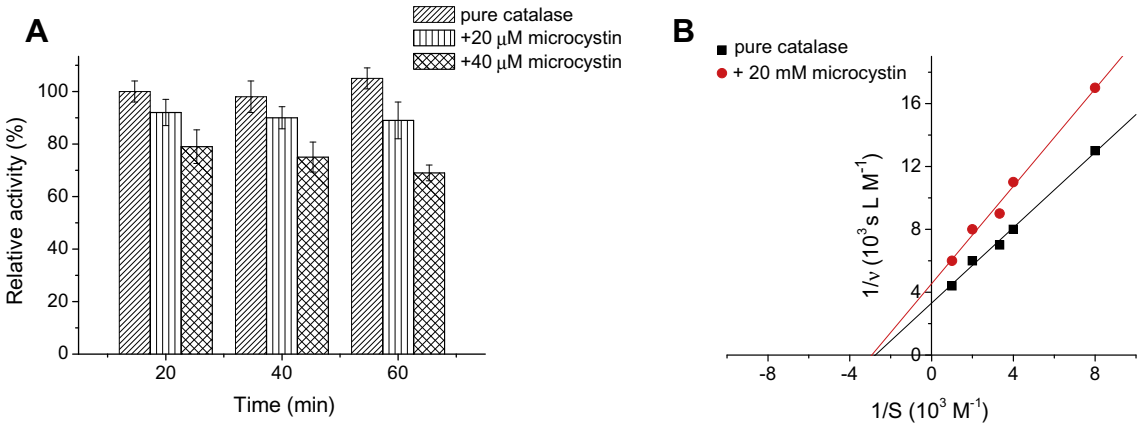

Fig. 8. (A) Effect of microcystin on catalase activity with exposure time to graded concentrations of microcystin for 20, 40 or 60 min. (B) (A) Lineweaver–Burk plots of catalase (5×10^{-6} M) in the presence and absence of microcystin. Data were pooled from at least three independent experiments.

hinders the binding of the enzyme substrate, leading to the enzyme inhibition.

Effect of the temperature on the fluorescence emission of catalase–microcystin bioconjugate

It is clear that body temperature has an important influence on the properties of proteins in biological environment as well as on the conjugation and interaction of proteins with drug ligands. We investigated the effect of the temperature on the fluorescence emission of catalase and catalase–microcystin bioconjugate by varying the temperature from 283 K to 353 K. Furthermore, it is well known that intrinsic fluorescence of tryptophan residue is highly sensitive to the microenvironment and, therefore, is widely used to investigate changes in the protein structure. It was seen that by increasing the temperature, the intensity of the emission was decreased. This behavior could be explained in terms of decreases of the quantum yield of the protein as a function of temperature mainly attributed to temperature-induced unfolding of protein. In addition, the influence of temperature on the

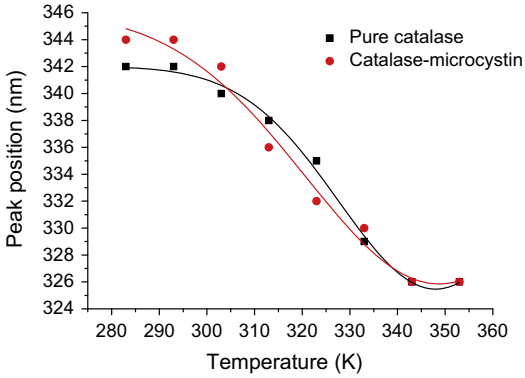

Fig. 9. Peak position transition of catalase–microcystin fluorescence emission. Concentrations of both catalase and microcystin are 2×10^{-6} M; pH 7.4.

fluorescence peak positions of pure catalase and catalase–microcystin was studied, and the results are represented in Fig. 9. A blue shift in the catalase emission peak position is observed by increasing the temperature. The changes in emission wavelength versus temperature represent two limiting regions. One was at the temperature lower than 293 K, that the wavelength of maximum emission is located at 342 nm, corresponding to native state of protein. The second was at temperatures higher than 343 K where the peak position of the protein blue-shifted to 326 nm, consistent with protein unfolded form. At intermediate temperatures (between 293 K and 343 K) a decrease in emission wavelength was observed, representing a transition from unfold to denature state of catalase. It should be emphasized again that the variation in the peak position could reflect the protein conformation changes. The catalase–microcystin solution represented a similar behavior in its temperature-induced denaturation curve. However, it is clear that slope of transition region (between 293 K and 343 K) is slightly bigger in temperature-induced denaturation curve of catalase–microcystin in comparison with pure catalase curve. This temperature study implies that the binding of microcystin to catalase inserted an effect on the thermal behavior of catalase.

Conclusion

In the present work, the interaction between microcystin and catalase was investigated employing different spectroscopic (fluorescence, CD, FT-IR) methods and enzymatic reactionkinetic techniques. The experimental results indicated that the microcystin binds to catalase with moderate affinity and the intrinsic fluorescence of catalase was quenched through static quenching mechanism. The binding parameters were calculated using the Stern–Volmer equation. The thermodynamic parameters, negative value of ΔH°, positive value of ΔS° and the negative value of ΔG° indicate that electrostatic interaction plays a major role in the binding process. The distance (r) between Trp-214 of catalase and microcystin was evaluated as $r = 2.86$ nm, following Forster non-radioactive resonance energy-transfer theory. Furthermore, CD and FT-IR evidences show that the secondary structure of catalase was changed after microcystin was bound to catalase. Our results may provide valuable information to understand the mechanistic pathway of toxicological behavior of microcystin.

Acknowledgments

This research was supported in part by the Fundamental Research Funds for the Central Universities (DL11BB20, DL10BB16) and Daqing Science and Technology Agency Science and Technology Program (SGG2009-068).

Appendix A. Supplementary material

Supplementary data associated with this article can be found, in the online version, at http://dx.doi.org/10.1016/j.saa.2013.09.078.

References

[1] A. Zehnder, P.R. Gorham, Canadian Journal of Microbiology 6 (1960) 645–660.
[2] T.W. Davis, D.L. Berry, G.L. Boyer, C.J. Gobler, Harmful Algae 8 (2009) 715–725.
[3] E.M. Jochimsen, W.W. Carmichael, J. An, D.M. Cardo, S.T. Cookson, C.E. Holmes, M.B. Antunes, D.A. de Melo Filho, T.M. Lyra, V.S.T. Barreto, New England Journal of Medicine 338 (1998) 873–878.
[4] B.J. Robson, D.P. Hamilton, Marine and Freshwater Research 54 (2003) 139–151.
[5] G. Zhang, P. Zhang, M. Fan, Ultrasonics Sonochemistry 16 (2009) 334–338.
[6] J. Kohoutek, P. Babica, L. Bláha, B. Maršálek, Analytical and Bioanalytical Chemistry 390 (2008) 1167–1172.
[7] A. Campos, V. Vasconcelos, International Journal of Molecular Sciences 11 (2010) 268–287.
[8] L.L. Amado, M.L. Garcia, P.B. Ramos, R.F. Freitas, B. Zafalon, J.L.R. Ferreira, J.S. Yunes, J.M. Monserrat, Science of the Total Environment 407 (2009) 2115–2123.
[9] R. Nishiwaki-Matsushima, S. Nishiwaki, T. Ohta, S. Yoshizawa, M. Suganuma, K.i. Harada, M.F. Watanabe, H. Fujiki, Cancer Science 82 (1991) 993–996.
[10] R. Dawson, Toxicon: Official Journal of the International Society on Toxinology 36 (1998) 953.
[11] X.C. Zhao, R.T. Liu, Environment International 40 (2012) 244–255.
[12] I. Moreno, S. Pichardo, A. Jos, L. Gomez-Amores, A. Mate, C. Vazquez, A. Camean, Toxicon: Official Journal of the International Society on Toxinology 45 (2005) 395.
[13] F. Ding, X.-N. Li, J.-X. Diao, Y. Sun, L. Zhang, L. Ma, X.-L. Yang, Y. Sun, Ecotoxicology and Environmental Safety 78 (2012) 41–49.
[14] H. Lineweaver, D. Burk, Journal of the American Chemical Society 56 (1934) 658–666.
[15] Y.J. Hu, Y. Ou-Yang, C.M. Dai, Y. Liu, X.H. Xiao, Molecular Biology Reports 37 (2010) 3827–3832.
[16] C. Kanakis, P. Tarantilis, M. Polissiou, S. Diamantoglou, H. Tajmir-Riahi, Journal of Molecular Structure 798 (2006) 69–74.
[17] C.D. Kanakis, P.A. Tarantilis, H.A. Tajmir-Riahi, M.G. Polissiou, Journal of Agricultural and Food Chemistry 55 (2007) 970–977.
[18] X. Zhao, R. Liu, Y. Teng, X. Liu, Science of the Total Environment 409 (2011) 892–897.
[19] A.Y. Khan, M. Hossain, G.S. Kumar, Chemosphere 87 (2012) 775–781.
[20] D.L. Andrews, Chemical Physics 135 (1989) 195–201.
[21] N. Tayeh, T. Rungassamy, J.R. Albani, Journal of Pharmaceutical and Biomedical Analysis 50 (2009) 107–116.
[22] Y. Yue, X. Chen, J. Qin, X. Yao, Dyes and Pigments 83 (2009) 148–154.
[23] G. Paramaguru, A. Kathiravan, S. Selvaraj, P. Venuvanalingam, R. Renganathan, Journal of Hazardous Materials 175 (2010) 985–991.
[24] J. Lloyd, Nature 231 (1971) 64–65.
[25] A. Belatik, S. Hotchandani, J. Bariyanga, H. Tajmir-Riahi, European Journal of Medicinal Chemistry 48 (2012) 114–123.
[26] X. Zhao, F. Sheng, J. Zheng, R. Liu, Journal of Agricultural and Food Chemistry 59 (2011) 7902–7909.
[27] P. Bourassa, J. Bariyanga, H.-A. Tajmir-Riahi, The Journal of Physical Chemistry B (2013).
[28] X.C. Zhao, R.T. Liu, Z.X. Chi, Y. Teng, P.F. Qin, Journal of Physical Chemistry B 114 (2010) 5625–5631.
[29] M. Xu, Z. Sheng, W. Lu, T. Dai, C. Hou, Journal of Biochemical and Molecular Toxicology 26 (2012) 493–498.
[30] Z. Xia, J. Jing, Journal of Molecular Structure 882 (2008) 96–100.
[31] A. Belatik, S. Hotchandani, R. Carpentier, H.-A. Tajmir-Riahi, Plos One 7 (2012) e36723.
[32] A.K. Sinha, Analytical Biochemistry 47 (1972) 389–394.
[33] L.H. Johansson, L. Håkan Borg, Analytical Biochemistry 174 (1988) 331–336.